



*Dedicated to the memory of
Professor Victor-Emanuel Sahini (1927–2017)*

GREEN SYNTHESIS OF COBALT FERRITE NANOPARTICLES USING PLANT EXTRACTS

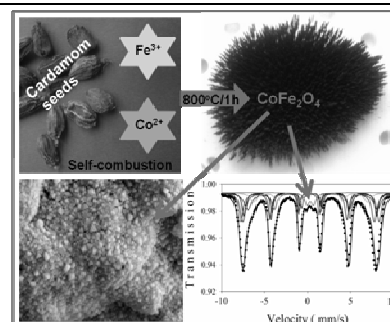
Dana GINGAȘU,^{a*} Ioana MÎNDRU,^a Silviu PREDA,^a Jose Maria CALDERON-MORENO,^a
Daniela C. CULIȚĂ,^a Luminița PATRON^a and Lucian DIAMANDESCU^b

^a Ilie Murgulescu Institute of Physical Chemistry, Roumanian Academy, 202 Splaiul Independenței, 060021 Bucharest, Roumania

^b National Institute of Materials Physics (NIMP), Atomistilor Street, No. 405A,
P. O. Box MG-7, Bucharest – Magurele 077125, Roumania

Received 14 December 2016

Cobalt ferrites nanoparticles (CoFe_2O_4) were synthesized through self-combustion method using aqueous extracts of ginger root and cardamom seeds. X-ray diffraction (XRD), scanning electron microscopy (SEM), infrared spectroscopy (IR) and Mössbauer spectroscopy were used for the characterization of the cobalt ferrite nanoparticles. X-ray diffraction patterns indicated the formation of the cubic phase CoFe_2O_4 . SEM micrographs revealed different morphological features of obtained cobalt ferrites. The Mössbauer parameters together with the inversion parameter and the cationic distribution were obtained from Mössbauer spectra recorded at room temperature.



INTRODUCTION

The magnetic nanomaterials have attracted an increased attention due to their potential applications as high-density magnetic recording media, as catalysts, as microwave absorbers.¹⁻³ In the biomedical field, they are used as carriers for drug delivery, as substrates in cancer treatment methods, as biosensors and, also, in magnetic resonance imaging.^{4,5}

Cobalt ferrite (CoFe_2O_4), a hard magnetic material, one of the important member of the spinel family has gained renewed interest due to its special physical and mechanical properties and implicit, to its new applications in lithium ion

batteries, magnetic photocatalysis and hyperthermia treatment.^{6,7} Due to its chemical, thermal and colour stability, cobalt ferrite nanoparticles are widely used in the ceramics industry as black colouring agents.⁸

Current trend in nanotechnology is the improvement of nanoparticles synthesis methods making them more efficient, simple and clean, thus reducing the environmental pollution.

The biogenic routes are an attractive alternative to the traditional synthesis methods. They are environmentally friendly, using nontoxic and biocompatible reagents, relatively reproducible and leading to materials with superior properties.⁹

* Corresponding author: d_gingasu@yahoo.com

Among the biological agents, plants seem to be the best candidates because of the vast reserves, easy accessible, widely distributed.¹⁰

The reactivity of plant extracts is due to their chemical composition, a combination of biomolecules such as polysaccharides, carbohydrates, phenols, flavonoids, terpenoids, amino acids, etc., which can act as capping agents, reducing/stabilizing and chelating agents.^{11,12}

The most important factors affecting the biosynthesis of the nanoparticles are undoubtedly the interactions of biomolecules with aqueous metal ions, the pH of the reaction medium, the reaction temperature and time.¹³

A large number of plant extracts are used especially to obtain noble metal nanoparticles, such as Ag, Au, Pt, Pd.^{10,13,14}

There are only a few studies on the biosynthesis of magnetic spinel ferrite nanoparticles using *Aloe vera*, *Hibiscus rosa-sinensis* leaf and sesame seed extract, respectively.¹⁵⁻¹⁸ No data on the synthesis of CoFe₂O₄ nanoparticles using ginger root extract or cardamom seeds extract.

Ginger (*Zingiber officinale*) and cardamom (*Elettaria cardamomum*) are two members of *Zingiberaceae* family.

Phenylpropanoid, zingerone, gingerol, oxalic acid, ascorbic acid are the main chemical components of ginger. Zingerone is the key component of the pungency of ginger.

Gingerol, shogaol and diarylheptanoids have antioxidant, anti-inflammatory and anti-diabetic activity.¹⁹

Cardamom, the Queen of all spices, "has a history as old as human race".²⁰ Seeds from cardamom have antibacterial gram-negative bacterium activity.

Cardamom contains a wide variety of phenolic compounds including gallic acid, ferulic, isoferulic acid, chlorogenic acid, caffeic acid, luteolin acid, quercetin, rutin, etc. Cardamom seeds have a warm, slightly pungent and highly aromatic flavour.²¹

The current study had the following goals: (i) the synthesis of cobalt ferrite nanoparticles (CoFe₂O₄) by self-combustion using ginger root and cardamom seeds aqueous extracts, respectively; (ii) the physico-chemical characterization of cobalt ferrite nanoparticles.

EXPERIMENTAL

Materials

The iron nitrate (Fe(NO₃)₃·9H₂O) and the cobalt nitrate (Co(NO₃)₂·6H₂O) were of reagent quality (Merck). Ginger

root and cardamom seeds were from the health food store originated in India.

Preparation of ginger root extract

20 g of ginger root were cutted and were placed in 100 ml distilled water. The mixture was boiled 5 min until the colour of the aqueous solution becomes yellow (pH ~ 6). The extract was cooled at room temperature and filtered.

Preparation of cardamom seeds extract

10 g of cardamom seeds are grinded in a coffee mill. The yellow-brown powder was placed in 100 ml distilled water under stirring. The mixture was boiled 4 h and then was filtered. The brown extract (pH ~ 6) was cooled at room temperature.

Self-combustion synthesis of CoFe₂O₄

The metal nitrates (2Fe³⁺:1Co²⁺) were added slowly under stirring to the aqueous ginger root/cardamom seeds extract, respectively. The precursor mixtures (pH ~ 2) were brought to a gel-like concentration in an oven at 80 °C. The gels were placed on a heater at 250-300 °C. Initially, the gels melted and, then, decomposed by spontaneous self-ignition, leaving behind magnetic foams.

The self-combustion reaction is an exothermic redox process in which the mixture of nitrates and plant extracts behave similarly to conventional oxidants and fuels.

The magnetic foams were calcined at 800 °C/1h to improve the degree of crystallization.

Characterization techniques

The diffractometer was set in parallel beam geometry, using Cu K α radiation ($\lambda = 1.5406 \text{ \AA}$), CBO optics and graphite monochromator, and operated at 40 kV and 30 mA, 0.02° step size and 5° min⁻¹ scan speed. Phase identification was performed using Rigaku's PDXL software, connected to ICDD PDF-2 database. The lattice constants were refined using Whole Powder Pattern Fitting (WPPF) and crystallite size was calculated by Williamson-Hall method.

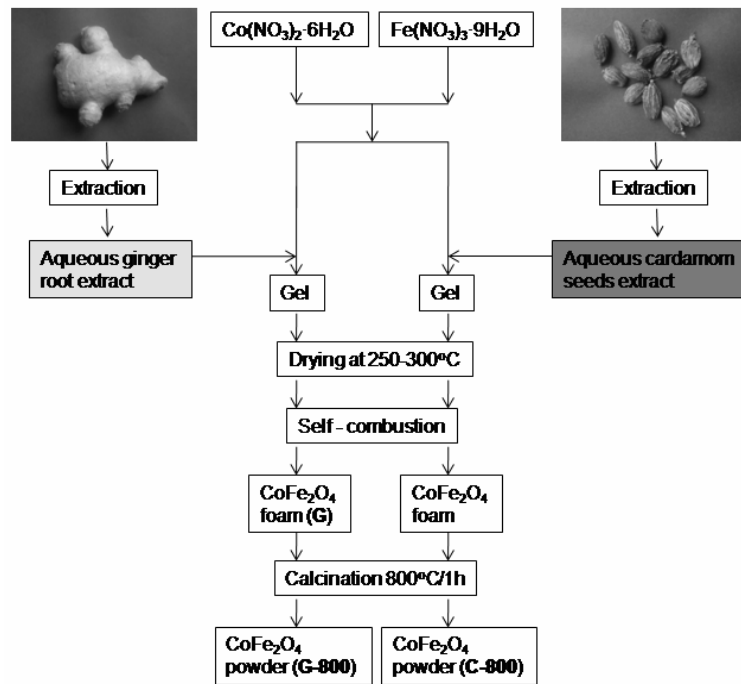
The microstructure of the oxidic powders was studied by scanning electron microscopy (SEM) in a FEI Quanta 3D FEG apparatus operating at voltages between 5 kV and 20 kV, using secondary electrons (SE) and equipped with an energy dispersive X-ray (EDX) spectrometer for elemental analysis.

The IR spectra of the cobalt ferrite powders were recorded on KBr pellets with a JASCO FTIR 4100 spectrophotometer in the 4000–400 cm⁻¹ wavenumber range.

Room temperature Mössbauer spectra were recorded by means of WissEL-ICE Oxford Mössbauer cryomagnetic system, with 20 mCi Co(Rh) γ -ray source, in a velocity range of ± 10 mm/s.

RESULTS AND DISCUSSION

The cobalt ferrite nanoparticles (CoFe₂O₄) were obtained through self-combustion method^{22,23} in which the chemical components from ginger root/cardamom seeds aqueous extracts act as chelating/reducing agents and, even, as fuel (Scheme 1).



Scheme 1 – Overall description for the preparation of CoFe_2O_4 through green synthesis method.

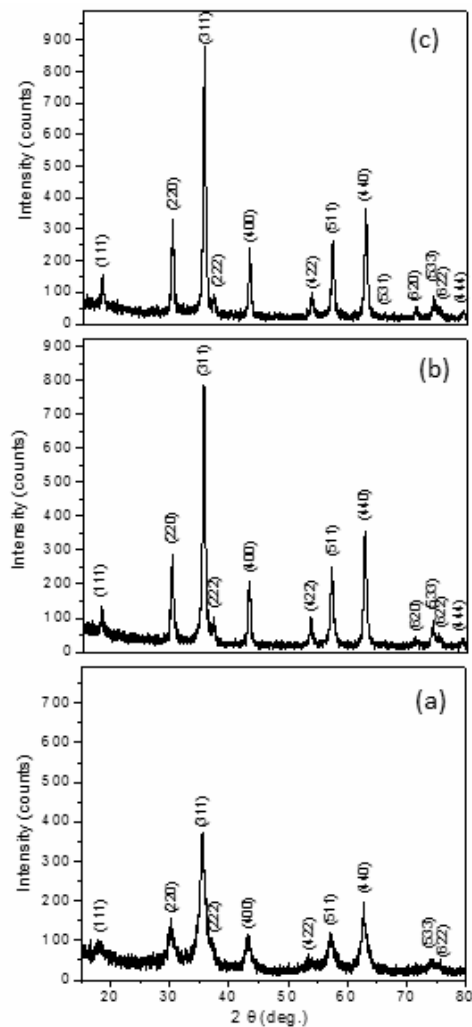


Fig. 1 – X-ray diffraction of the cobalt ferrites obtained by self-combustion using ginger root/cardamom seed extracts: (a) G, (b) G-800, (c) C-800.

The formation of cobalt ferrites was confirmed from XRD patterns (Fig. 1). The X-ray diffraction pattern of the oxide powder obtained from self-combustion reaction using the aqueous extract of ginger root confirmed the formation of CoFe_2O_4 (**G**) with cubic structure (ICDD 022-1086, space group $\text{Fd}\bar{3}\text{m}$), (Fig. 1a). To improve the crystallinity degree of the powder, an additional treatment of 1h at 800 °C (**G-800**) was used (Fig. 1b). The X-ray diffraction of the cobalt ferrite prepared through the self-combustion reaction using the aqueous cardamom seeds extract and calcined at 800 °C/1h (**C-800**) is presented in Fig. 1c. Single phase spinel CoFe_2O_4 was confirmed for all these samples.

The lattice parameters of the CoFe_2O_4 samples are: 8.350 Å (**G**), 8.348 Å (**G-800**) and 8.360 Å (**C-800**), in good agreement with the literature.^{24,25} The average crystallite size was as following 49.4 Å (**G**), 123.6 Å (**G-800**) and 146.7 Å (**C-800**).

The microstructure of the samples was studied by scanning electron microscopy. SEM micrographs of the sample **G** (Fig. 2) revealed the formation of agglomerates with a very fine nanograined structure containing equiaxed nanocrystals (~ 30 nm).

SEM measurements of the sample **G-800** (Fig. 3) show the formation of porous agglomerates with nanograined structure, the majority remaining equiaxed ~ 30 nm and only a few becoming faceted crystals with crystal size ~ 100 nm.

The morphology of the sample **C-800** (Fig.4) evidenced fine grained agglomerates with well-defined faceted crystals (crystal size ~ 100 nm).

EDX spectroscopy detected in the samples obtained using ginger root extract (**G**, **G-800**), the presence of C, P, S, K as minor elements; all these elements are present in the ginger root extract, the major component (~ 95 wt%) being the elements of CoFe_2O_4 nanocrystallites.

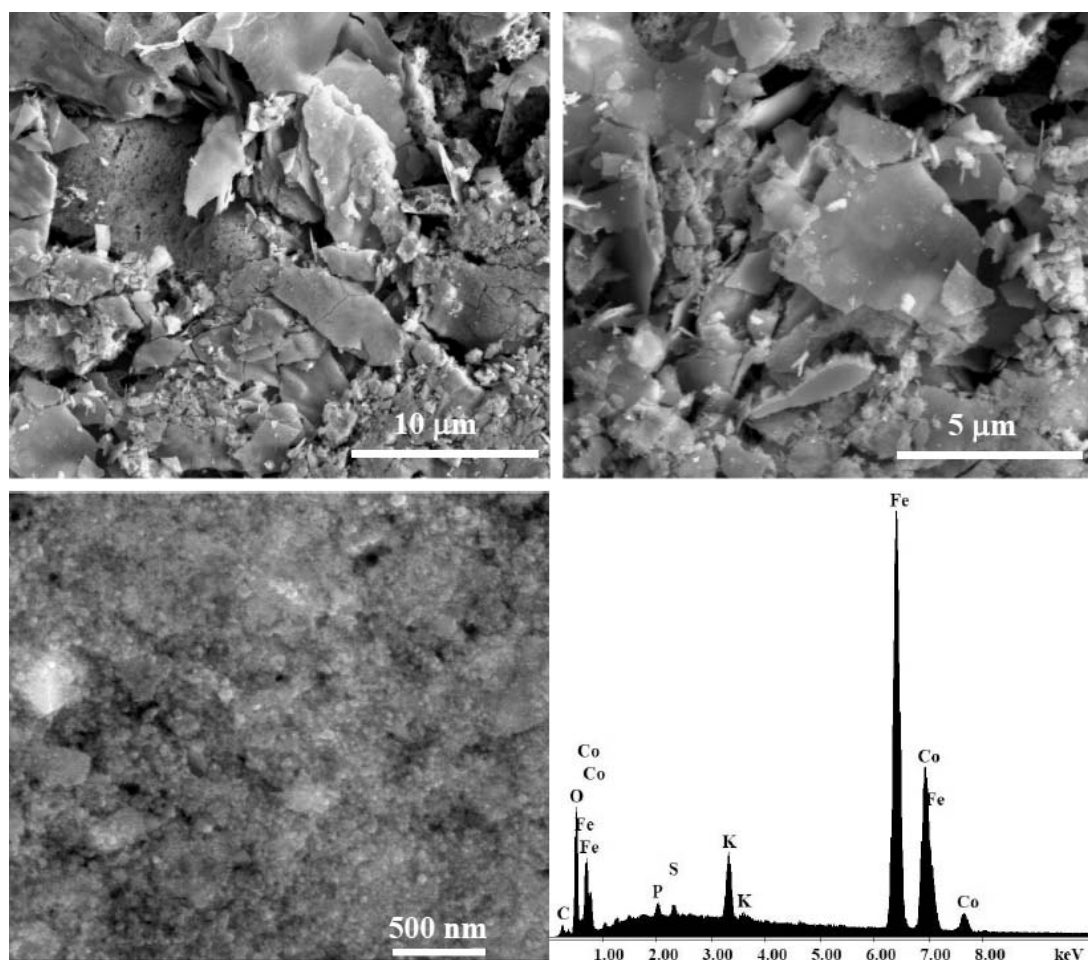


Fig. 2 – SEM micrographs, at different magnifications, and EDX spectrum of the sample **G** obtained by self-combustion using ginger root extract.

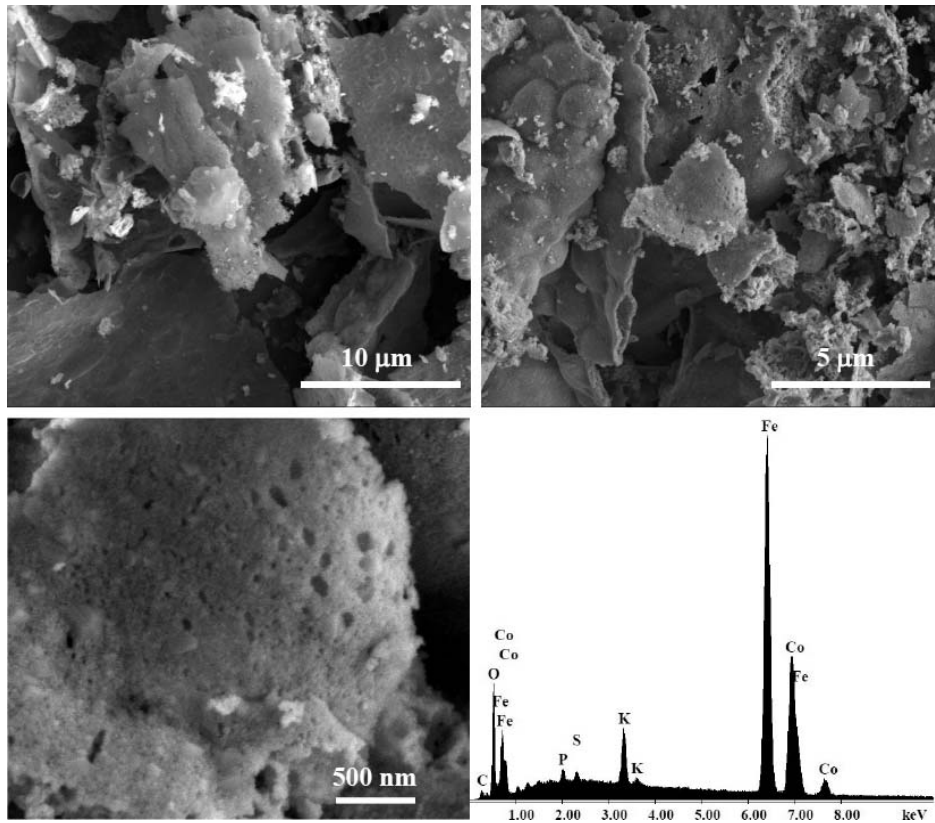


Fig. 3 – SEM micrographs, at different magnifications, and EDX spectrum of the sample **G-800** obtained by self-combustion using ginger root extract and calcined at 800 °C/1h.

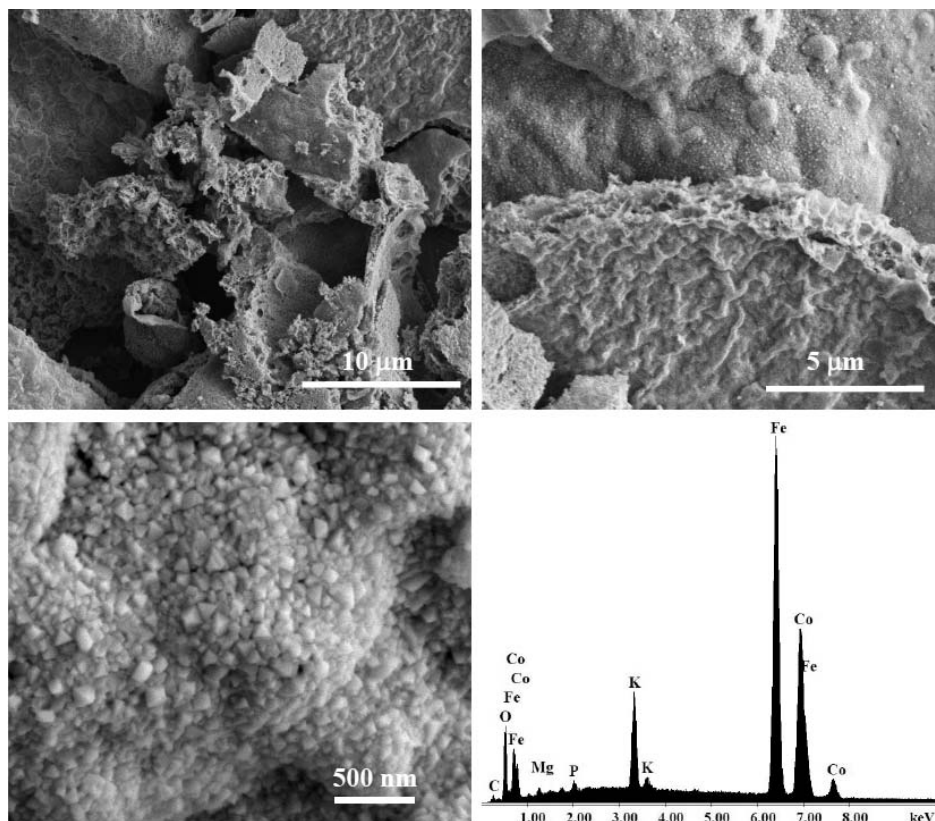


Fig. 4 – SEM micrographs, at different magnifications, and EDX spectrum of the sample **C-800** obtained by self-combustion using cardamom seeds extract, calcined at 800 °C/1h.

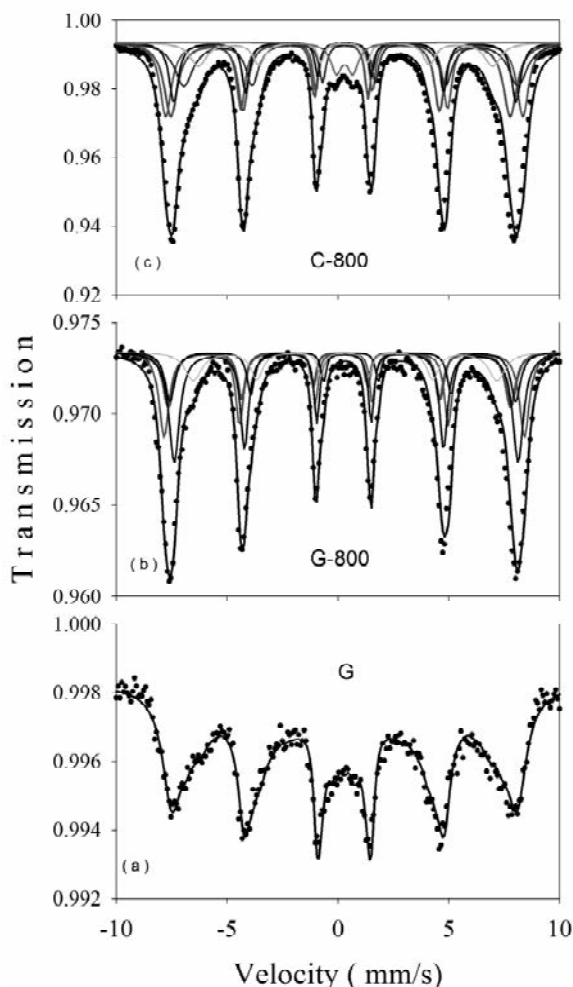


Fig. 5 – Mössbauer spectra of the synthesized cobalt ferrite samples: (a) G, (b) G-800, (c) C-800. Continuous lines represent the fit with experimental points.

In the CoFe_2O_4 sample obtained using cardamom seeds extract (**C-800**), EDX spectroscopy evidenced the presence of K, Mg and P, all of them being cardamom seeds chemical components and the elements of CoFe_2O_4 (~ 96 wt%).

The Mössbauer spectra of the synthesized samples were recorded at room temperature. The sample thickness was calculated at $\sim 7 \text{ mg cm}^{-2}$ in order to avoid additional contributions to the line width. In Figs. 5(a-c) the obtained spectra are presented together with the computer fit (continuous lines) in the hypothesis of Lorentzian lines. All spectra exhibit magnetic hyperfine sextets. A small additional doublet (~ 4% from the total area) coming from very small particles can be observed in the sample **C-800**.

In order to understand the presented deconvolution of Mössbauer spectra we have to remember some basic elements regarding the structure of spinel oxides. The general formula, reflecting the cation distribution of a spinel oxide

can be written as $(\text{M}_{1-x}\text{Fe}_x)_{\text{Td}}[\text{M}_x\text{Fe}_{2-x}]_{\text{Oh}}\text{O}_4$ where Td and Oh means tetrahedral and respectively octahedral cation sites in the lattice. The site occupancy of cations is strongly related to the synthesis method and thermal history of the sample.²⁶ In a spinel oxide each octahedral site has six tetrahedral cations as the second nearest neighbours. In a complete inverse spinel ($x=1$) all divalent cations can be found in octahedral sites. In cobalt ferrite - a partial inverse spinel, cobalt ions can be found also in tetrahedral site, changing the configuration of Fe^{3+} in octahedral sites. This structural peculiarity changes the hyperfine fields at octahedral positions *via* supertransferred hyperfine interactions generating an increase in the Mössbauer line widths of Fe^{3+} at octahedral sites. With the assumption of a random distribution of Fe^{3+} and Co^{2+} in tetrahedral sites, the intensity of each subspectra of octahedral sites are given by a binomial distribution probability.²⁷

The best fit for the **G** sample was obtained assuming a hyperfine magnetic field distribution (Fig. 5a). The magnetic field distribution is rather large, from 4T to 48T, (Table 1) suggesting a large nanoscaled particle size distribution and poor crystallization (Mössbauer effect is very low).

For the samples treated at 800 °C/1h (**G-800** and **C-800**) the best fit with the experimental points (Figs. 5b and 5c) was obtained considering one tetrahedral magnetic sublattice (Td) and four relevant octahedral sublattices O_{h0}, O_{h1}, O_{h2}, O_{h3} which correspond to the presence of 0, 1, 2 and 3 divalent cobalt ions in the tetrahedral positions of the spinel structure. The refinements of the spectra were performed with fixed line intensities ratio as 3:2:1 – the theoretical value for polycrystalline samples. The Mössbauer fit parameters isomer shift (IS), quadrupole splitting (ΔE_Q) and hyperfine magnetic field (H_{hf}) are listed in Table 1 together with the area ratio A_{Td}/A_{Oh} (A_{Td} and A_{Oh} are the areas corresponding to the tetrahedral and octahedral sites respectively). The tetrahedral sextet (continuous red lines in Figs. 5b and 5c) is characterised by lower IS and H_{hf} ²⁸ in good agreement with the local environment considerations.

The area ratio A_{Td}/A_{Oh} can reveal the cation distribution in the sample. Considering the formula $(Co_{1-x}Fe_x)_{Td}[Co_xFe_{2-x}]_{Oh}O_4$, the area ratio A_{Td}/A_{Oh} can be written as follows:

$$A_{Td}/A_{Oh} = x f_{Td} / (2-x) f_{Oh} \quad (1)$$

where f_{Td} and f_{Oh} are the Debye-Waller factors for Fe^{3+} in tetrahedral respectively octahedral positions. Since $f_{Td} = 1.2 f_{Oh}$, from the relation (1) we can obtain for the inversion parameter x the following relation:

$$x = 2A_{Td} / (1.2A_{Oh} + A_{Td}) \quad (2)$$

allowing as to determine this parameter from Mössbauer spectra. The stoichiometry of the analysed samples as resulted from Mössbauer data is shown in Table 2.

In order to sustain the formation of $CoFe_2O_4$ spinel structure, the FTIR spectra of ginger root and cardamom seeds aqueous extracts and of the cobalt ferrite samples are recorded in the range 4000-400 cm^{-1} . The assignments of bands are listed in Table 3 and are in good agreement with the literature data.^{29,30}

Table 1

Mössbauer fit results of $CoFe_2O_4$ samples (**G**, **G-800**, **C-800**)

Sample	IS* (mm/s)	ΔE_Q (mm/s)	H_{hf} (T)	Site / phase assignment	A_{Td}/A_{Oh}
G	0.356	0.007	3.62- 48.16	Hyperfine field distribution	
G-800	0.175	-0.046	47.71	T _d	0.19
	0.345	-0.015	50.21	O _{h0}	
	0.359	0.163	48.18	O _{h1}	
	0.395	0.095	47.91	O _{h2}	
	0.388	0.015	42.33	O _{h3}	
C-800	0.205	-0.031	46.88	T _d	0.39
	0.354	0.003	49.33	O _{h0}	
	0.263	0.013	47.29	O _{h1}	
	0.491	0.086	46.15	O _{h2}	
	0.378	0.060	40.66	O _{h3}	
	0.371	0.738	-	Superparamagnetic cobalt ferrite	
Errors	±0.002	±0.004	±0.02		

*IS is given relative to α -Iron.

Table 2

Normalised tetrahedral and octahedral areas together with the inversion parameter and cation distribution of the samples **G-800** and **C-800**

Sample	A_{Td}	A_{Oh}	x	Cation distribution $(Co_{1-x}Fe_x)[Co_xFe_{2-x}]O_4$
G-800	0.16	0.84	0.27	$(Co_{0.73}Fe_{0.27})[Co_{0.27}Fe_{1.73}]O_4$
C-800	0.27	0.69	0.49	$(Co_{0.51}Fe_{0.49})[Co_{0.49}Fe_{1.51}]O_4$

Table 3

The characteristic bands of the ginger root extract, cardamom seeds extract and CoFe₂O₄ samples

Ginger root extract	G	G-800	Cardamom seeds extract	C-800	Assignment
3394 vs	3200 w,br	3446 w	3413 vs	3370 m	vOH in water
2931 m, sh	-	-	2933 s, sh	-	vCH in phenols
2870 sh	-	-	-	-	vCH ₂ sym
1637 vs	-	-	1625 s	-	vC=O/vCOO ⁻ _{asym}
-	-	1625 w	-	1646 w	vOH
-	-	-	1415 m	-	vCOO ⁻ sym
-	1384 m	-	-	-	vNO ₃ ⁻
1384 vs	-	-	-	-	vbend CH to CH ₃
1309 sh	-	-	1250 w	-	vC-O-C asym
1151 sh	1120 w	-	1155 sh	-	vC-OH
1079 vs	-	-	1024 s	1014 m	vC-OH
1054 vs	-	-	-	-	vC-O-C sym
925 w	-	-	-	-	γCH ring vibration
782 w	-	-	-	-	γCH ring vibration
670 m	-	-	-	-	vCH ring vibration
-	574 vs	570 vs	-	587 vs	vFe-O (Td)
-	418 s	418 s	-	410 s	vFe-O (Oh) and vCo-O (Oh)

vs=very strong, s=strong, m=medium, w=weak, sh=shoulder, br=broad

The spectra of ginger root and cardamom seeds extracts show main bands of phenolic hydroxyl group (-OH) which represent hydrogen bonding in flavonoids and also, in water, C-H in CH₂ and in the phenyl ring, symmetric and asymmetric vibrations of C-O and C=O bonds in COO⁻ groups, stretching vibrations of benzene ring containing aromatic substituents.^{29,30}

The all spectra of CoFe₂O₄ evidence two very strong bands in the range of 800-400 cm⁻¹ assigned to the stretching vibrations of Fe-O bonds in the spinel structure: ν₁ at 574 cm⁻¹ (**G**), 570 cm⁻¹ (**G-800**), 587 cm⁻¹ (**C-800**) assigned to the stretching vibrations of Fe-O bond in the tetrahedral sites and ν₂ at ~ 418 cm⁻¹ assigned to the Fe-O and Co-O vibrations in the octahedral sites.³¹

CONCLUSIONS

A green chemistry synthesis of cobalt ferrite using ginger root /cardamom seeds aqueous extract was developed. The CoFe₂O₄ nanoparticles were obtained by self-combustion method in which the chemical components from ginger/cardamom extracts act as chelating/reducing agents and, also, as fuel. To the best of our knowledge, there are no literature data on the synthesis of CoFe₂O₄ using ginger root/cardamom seed aqueous extracts. XRD analysis demonstrated that self-combustion method using plant extracts has led to the formation of the

spinel-type CoFe₂O₄ with good crystallinity for **G-800** and **C-800** samples. The morphology of the obtained cobalt ferrites was investigated by SEM measurements. The EDX spectra evidenced the presence of the elements of cobalt ferrite, along with C, K, P, S and Mg as minor elements, associated with the elemental content of the plant extracts. In good agreement with XRD measurements, the Mössbauer spectra confirm the formation of cobalt ferrite spinel and the relevance of thermal treatment for structure stabilisation. Moreover, the Co²⁺ and Fe³⁺ cation distribution was evidenced showing a higher preference of Co²⁺ ions for tetrahedral sites in the sample **G-800**. It can be noticed that the cation distribution was influenced by the nature of the plant extract (x=0.27/0.49 for **G-800/C-800**). These results demonstrated that the use of aqueous ginger/cardamom extracts in the green chemistry synthesis of CoFe₂O₄ nanoparticles is a promising and eco-friendly alternative.

Acknowledgments: Support of the European Union (ERDF) and of the Romanian Government under the POS-CCE O 2.2.1 project INFRANANOCHEM - Nr. 19/01.03.2009, allowing for the acquisition of the research infrastructure, is gratefully acknowledged. The work also benefits from the support of the "Materials Science and Advanced Characterization Methods" Programme of the "Ilie Murgulescu" Institute of Physical Chemistry, financed by the Roumanian Academy. One of the authors (L.D.) greatly acknowledges the financial support under the Core Program PN 10N.

REFERENCES

1. D.E. Speliotis, *J. Magn. Magn. Mater.*, **1999**, *193*, 29-35.
2. L.M. Rossi, N.J.S. Costa, F.P. Silva and R. Wojcieszak, *Green Chem.*, **2014**, *16*, 2906-2933.
3. D.H.K. Reddy and Y.-S. Yun, *Coord. Chem. Rev.*, **2016**, *315*, 90-111.
4. P.C. Morais, *J. Alloys Compds.*, **2009**, *483*, 544-548.
5. D. Alcántara, S. Lopez, M.L. García-Martin and D. Pozo, *Nanomedicine: NBM*, **2016**, *12*, 1853-1862.
6. S. Amiri and H. Shokrollahi, *Mater. Sci. Eng. C*, **2013**, *33*, 1-8.
7. Y.-Q. Chu, Z.-W. Fu and Q.-Z. Qin, *Electrochim. Acta*, **2004**, *49*, 4915-4921.
8. H. Yüngevis and E. Ozel, *Ceram. Int.*, **2013**, *39*, 5503-5511.
9. O.V. Kharissova, H.V.R. Dias, B.I. Kharisov, B.O. Pérez and V.M.J. Pérez, *Trends Biotechnol.*, **2013**, *31*, 240-248.
10. A. Schröfel, G. Kratošová, I. Šafařík, M. Šafaříková, I. Raška and L.M. Shor, *Acta Biomater.*, **2014**, *10*, 4023-4042.
11. I.M. Chung, I. Park, K. Seung-Hyun, M. Thiruvengadam and G. Rajakumar, *Nanoscale Res. Lett.*, **2016**, *11*, 40-45.
12. S. Ahmed, M. Ahmad, B.L. Swami and S. Ikram, *J. Adv. Research.*, **2016**, *7*, 17-28.
13. M. Shah, D. Fawcett, S. Sharma, S.K. Tripathy and G.E.J. Poinern, *Materials*, **2015**, *8*, 7278-7308.
14. A.K. Mittal, Y. Chisti and U.C. Banerjee, *Biotechnology Adv.*, **2013**, *31*, 346-356.
15. A. Manikandan, R. Sridhar, S.A. Antony and S. Ramakrishna, *J. Mol. Struct.*, **2014**, *1076*, 188-200.
16. S. Phumying, S. Labuayai, E. Swatsitang, V. Amornkitbamrung and S. Maensiri, *Mater. Res. Bull.*, **2013**, *48*, 2050-2065.
17. P. Laokul, V. Amornkitbamrung, S. Seraphin and S. Maensiri, *Curr. Appl. Phys.*, **2011**, *11*, 101-108.
18. D. Gingasu, I. Mindru, O.C. Mocioiu, S. Preda, N. Stanica, L. Patron, A. Ianculescu, O. Oprea, S. Nita, I. Paraschiv, M. Popa, C. Saviuc, C. Bleotu and M.C. Chifiriuc, *Mater. Chem. Phys.*, **2016**, *182*, 219-230.
19. H.A. Hasan, A.M.R. Rauf, B.M.A. Razik and B.A.R. Hassan, *Pharam. Anal. Acta.*, **2012**, *3*, 1000184 (5 pages).
20. K.P. Amma, P. Amma, M.P. Rani, I. Sasidharan and V.N.P. Nisha, *Intern. J. Biol. Med. Research*, **2010**, *1*, 20-24.
21. O.V. Evdokimova, I. Tarrab, E.V. Neneleva and I.Y. Glazkova, *Eur. J. Appl. Sci.*, **2013**, *5*, 142-145.
22. D. Gingasu, L. Diamandescu, I. Mindru, G. Marinescu, D.C. Culita, J.M. Calderon-Moreno, S. Preda, C. Bartha and L. Patron, *Croat. Chem. Acta*, **2015**, *88*, 445-451.
23. D. Gingasu, I. Mindru, L. Patron, J.M. Calderon-Moreno, O.C. Mocioiu, S. Preda, N. Stanica, S. Nita, N. Dobre, M. Popa, G. Gradisteanu and M.C. Chifiriuc, *J. Nanomater.*, **2016**, Article ID 2106756, (12 pages).
24. A.B. Salunkhe, V.M. Khot, M.R. Phadatare and S.H. Pawar, *J. Alloys Compds.*, **2012**, *514*, 91-96.
25. P.C. Rajath Varma, R.S. Manna, D. Banerjee, M.R. Varma, K.G. Suresh and A.K. Nigam, *J. Alloys Compds.*, **2008**, *453*, 298-303.
26. Z.J. Zhang, Z.L. Wang, B. Chakoumoks and J.S. Yin, *J. Am. Chem. Soc.*, **1998**, *120*, 1800-1804.
27. G.A. Sawatzky, F. Van Der Woude and A.H. Morrish, *Phys. Rev.*, **1969**, *187*, 747-757.
28. G.S.N. Rao, B.P. Rao and H.H. Hamdeh, *Proced. Mater. Sci.*, **2014**, *6*, 1511-1515.
29. A.D. Matter Al-Maliki, *J. Missan Res.*, **2011**, *8*, 13-34.
30. H. Purnomo, F. Jaya and S.B. Widjanarko, *Intern. Food Res. J.*, **2010**, *17*, 335-347.
31. R. Safi, A. Ghasemi, R. Shoja-Razavi and M. Tavousi, *J. Magn. Magn. Mater.*, **2015**, *396*, 288-294.

